Available on CMS information server

CMS NOTE 1997/022

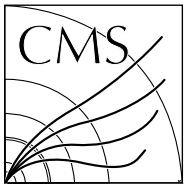

The Compact Muon Solenoid Experiment

CMS Note

Mailing address: CMS CERN, CH-1211 GENEVA 23, Switzerland

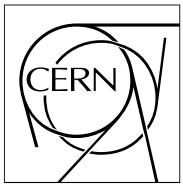

June 19, 1997

Study of Analogue Signal Processing Algorithms for MSGC Signals in CMS

F. G. Sciacca

Imperial College of Science Technology & Medicine, London, UK

Abstract

Several analogue signal processing algorithms for associating an MSGC signal to a beam crossing interval (BCI) at the LHC frequency have been evaluated and compared using different sets of signals, both simulated and from a beam test, with the purpose of indicating the most suitable for implementation in the front end readout chip.

Issues of performance and practical implementation within the proposed readout scheme for the CMS tracker are discussed.

1 Introduction

At LHC interactions occur every 25ns at each beam crossing. A good track reconstruction efficiency in the central detector demands a minimum pile-up of hits coming from interactions occurring in different bunch crossing intervals. Therefore it is essential to be able to associate a signal in the preamplifier with the correct beam crossing slot. The approach of using a pulse shaping time longer than the interval between subsequent beam crossings has been chosen for the silicon tracking detector. The aim of the analogue processing is to extract from the slow shaped pulse most of the information from the original MSGC signal with the best possible efficiency and timing resolution.

In the case of the silicon detectors the signal is shaped with a characteristic time of 50 ns, then it is sampled at the beam crossing frequency and stored in an analogue delay buffer. When a trigger occurs an analogue pulse shape processor (APSP) uses three samples of the preamplifier output to reconstruct the signal generated by the detector with an amplitude efficiency close to 100% for signals exactly in phase with the LHC clock and a timing resolution of one BCI [1-4]. The method is effective because the signals from silicon detectors approximate very well an ideal delta impulse and the shaped pulse can be considered an ideal CR-RC pulse. This approach, developed by the RD20 collaboration, has been implemented in the APV series, the front-end readout chip for the silicon micro strip tracker [5].

The MSGC signals instead are characterised by large fluctuations in size and duration. Besides this, the time origin of the signal depends strongly on the point in the detector where the first electron-ion pair is generated. The overall time evolution of the signals is strongly affected by statistical fluctuations of different quantities that are in turn determined by the choice of the geometry and configuration of the detector: gas gap, gas gain, cathode voltage, drift velocity of charges in the gas [6]. The shaped signal can no longer be considered a CR-RC pulse and the elementary deconvolution operation does not confine the signal to a single BCI nor recover the full amplitude of the detector signal.

However, since some features of the MSGC detectors are very similar to those of silicon detectors, it is foreseen to adapt the APV front-end chip to the readout of the MSGCs. Modifications are required for the analogue signal processor in order to account for the differences outlined above. The aim of this study is to compare the performance of different processing methods for the MSGCs signals in different scenarios in order to isolate those whose performance is most consistently close to the CMS requirements. In order to achieve this, I simulated in software several different processing algorithms and I have used three different sets of signals to assess their performance:

a) simplified simulated signals which take into account some general properties of MSGC signals and not the specific detector configuration;

b) simulated signals for a specific detector geometry and configuration;

c) signals from a beam test.

2 Description of the Problem

An MSGC signal is the superimposition of several current signals each generated by one avalanche (Figure 1). A single avalanche signal is constituted by two components: a fast electron component which develops and decays within a few tenths of nanoseconds and accounts for about 10% of the total charge deposited and an ionic component which develops rapidly, but decays slowly (several tens of nanoseconds).

For a given detector configuration, the main factors that affect the fluctuations in the signal time evolution and amplitude are two: the size of signal varies for different avalanches and different avalanches reach the anode at different times. The latter factor dominates strongly. In the detector configurations proposed for CMS most of the charge is collected at the front end within two BCI.

From the point of view of the electronics the different factors affecting the time evolution of the signals generate the unwanted effect of shifting the peaking time of the shaped pulse, thus degrading the time resolution. Besides this the long charge collection time leads to a shaped signal which decays to zero very slowly generating pile-up effects which contribute to both the time resolution deterioration and to an increase in the detector occupancy. The analogue processing should be effective in minimizing both these effects.

3 Description of the Algorithms

Three different approaches to signal processing have been investigated and compared in this study. They are all based on the assumption that the signal is shaped with a time constant of 50 ns and then sampled at the beam crossing frequency and stored onto the analogue pipeline. It is also assumed that it will be possible to phase the sampling time conveniently with respect to the LHC clock in order to optimise performance. All results presented in the following sections are obtained after optimising in 5 ns steps within a 2 BCI time interval.

- The first method is derived directly from the deconvolution method, and consists in generating a weighted sum of a number of samples of the shaped pulse. This approach has been studied in some detail over the past years [7, 8] and several combinations of weights optimized according to different criteria have been investigated. I have picked up from this work the most significant algorithms and slightly modified some of them for further investigation. I will refer to this approach as *weighted sum*. A summary of the different sets of weights is reported in Table 1. The relative contribution to the noise of the front-end due to the algorithm implementation in the electronic circuitry is computable analytically [4] for the different cases and is also reported in the table. Figure 2 shows the weighting function [3] for some of the sets of weights considered.
- The second approach had been originally developed for the proposed MSGC for the ATLAS experiment [8, 9]. Assuming that a genuine preamplifier signal from a particle in the detector has a steep leading edge, the algorithm consists in comparing some linear combinations of samples of the shaped pulse against some thresholds in order to determine whether, at the trigger time a signal with a steep leading edge was present or not. I will call this method *edge-finding*.
- With the third approach it is assumed that the peak of the shaped signal carries the information about the signal timing. In this case the processor, following a trigger, determines whether the pulse shape is peaked where it is expected. I will refer to this method as *peak-finding*. A similar method has been evaluated in a different study [11].

  Table 2 summarizes the conditions required from both peak and edge finding filters. One can observe that the practical implementation of both is very similar, although the two methods are conceptually different. It should be remarked that a design for implementing such algorithms is not yet existent. In particular, the possibility of putting out the sample at the peak (denoted as *Vn*) has to be exploited.

4 Signals Used

4.1 Simplified Simulated Signals

The basic signal is a rectangular current pulse of duration 50 ns or 2 BCI arbitrarily normalised to unit charge. It can be thought as a succession of closely spaced delta current impulses and it is meant to represent a sort of average of several signals.

Different fluctuation effects can be incorporated in the model adding more signals generated by conveniently combining different rectangular pulse lengths and sizes. Delays with respect to the nominal trigger time are also introduced for each of the signals considered. A set of 30 signals is thus obtained, meant to represent a sort of worst possible scenario due to fluctuations or changes in the operating conditions of the detector (Figure 3).

4.2 Realistic Simulated Signals

A Monte Carlo program developed at Pisa [6] was used to generate 1000 signals from MIPs at perpendicular incidence. The program simulates current pulses obtained with a 3 mm chamber filled with Ne/DME (50/50) with an average gain of 2000. The charge is collected on one strip only and anode readout is considered with V_{an}=gnd, V_{cath}=-550 V, V_{drift}=-3.5 kV. The front end shaper is an ideal CR-RC with a time constant of 50 ns considering a detector capacitance of 20 pF. Electronic noise is not added to the signals (Figure 4).

4.3 Beam Test Signals [10]

2000 signals in four adjacent channels from perpendicularly incident particles recorded using a 3 mm chamber filled with DME/CF_4 (80/20). The front end electronics was constituted by the PRESHAPE32 with a shaping time of 40 ns. To compensate for this difference in the integration time with respect to the foreseen shaping time of 50 ns a sampling at 20 ns rather than at 25 ns has been applied in order to maintain the ratio between shaping and sampling time. Equally the sampling timing optimisation is done in steps of 4 ns within a 2 BCI interval.

Front end electronic noise (Figure 5) was estimated from calibration to be 1400 e^-. However, the accuracy of this calibration has not, to date, been verified. Cross-talk effects are visible on the average pulse shape of the channel that collects the smaller fraction of charge.

5 Criteria for Comparison

In order to compare the methods in a meaningful way three variables are defined which can be evaluated on the same grounds for each algorithm in the three categories.

Efficiency ε defined as the ratio to the number of triggers of hits associated with the correct BCI which pass a threshold cut. The "correct" BCI is chosen for each algorithm to be the one in which, on average, events are detected most efficiently.

Fake hits rate ϕ defined as the ratio of the number of hits passing the threshold cut but associated with a wrong BCI to the number of hits associated correctly·[1].

Signal gain γ defined as the ratio between the analogue values after and before the signal processing averaged over all the triggers.

Curves of efficiency and fake hits rate against threshold were generated for each algorithm using the three different sets of input signals. The threshold is expressed in terms of σ, defined to be the Equivalent Noise Charge (ENC) of the front end electronics. This is taken to be the ENC expected for the APV chip (1400 e^-) in the case of the simulated signals (which contain no noise) and the measured noise of the PRESHAPE32 (1400 e^-) for the beam test signals. In both cases the contribution to the ENC from the APSP (as listed on Table 1) has been added to the σ.

Efficiency was then plotted versus fake hits rate to produce a better visual representation of the performance behaviour with threshold[2].

Some caution has to be taken when interpreting the values of efficiency in the case of the beam test data, where signals from MIPs are shared by up to 4 channels, in contrast with the simulated signals for which the charge is supposed to be collected on a single strip. For the beam test data I have adopted the following criterion: for each channel I estimated the fraction of triggers yielded by a 3σ cut on the unprocessed signal (see figure 5) with σ not including the contribution to the noise due to the processing. I then referred to these values when looking at the post processing efficiency.

However, for the sake of a more direct visual comparison with the results from the simulated signals, I also processed the beam test signals obtained clustering the four channels and generated curves of efficiency vs fake hits rate in this case.

6 Discussion of Results

A preliminary selection of weighted sum algorithms has been carried out with a simple method. The filters were applied to two different input signals, the one generated by a single avalanche and the square pulse of the duration of two BCI. The weighted sum signals obtained in the two cases were compared and if they did not overlap for more than 50% of the area, the algorithm was discarded. The point is to keep those filters whose response is least dissimilar in the cases of two input signals which are completely different: they should be less affected by the fluctuations. Six weighted sum algorithms were discarded as a result of this selection.

Three more weighted sum filters have been discarded following the combined analysis of the three sets of inputs. They consistently yielded worse performance and the results are omitted from the plots for the sake of clarity.

---

[1] The fake hits rate is directly related to the time resolution for an isolated signal (time res $=\varepsilon*(\phi+1)$ in units of BCI) and the final occcupancy of the MSGCs, given the initial occupancy (final occ.=[initial occ]*[$\varepsilon*(\phi+1)$])

[2] Note that for the weighted sum filters s is a threshold which discriminates signal from noise; it is adjustable offline for each single channel at the stage where the zero suppression is performed. For edge and peak finding (both comparator based methods) it is a hardware threshold and it discriminates between different samples of the same signal. The implications of this difference are very important and they strongly affect performance.

For the remaining six algorithms the results referring to an isolated trigger are shown and discussed in the following sections. The six algorithms are those marked with a "*" in Table 1 and Table 2. Figure 6 shows the curves of efficiency Vs fake hits rate and Figure 8 illustrates the signal gain.

6.1 Efficiency vs Fake Hits Rate

It is evident from the three sets of results in figure 6 that processing the signals with the comparator based filters (Peak or Edge finding) yields quite different results compared with the different weighted sum processings. Therefore for the moment I will simply distinguish between the two groups. Further considerations about signal to noise ratio discussed in the next section will be used to discriminate between each individual filter.

Both the comparator based filters perform excellently in terms of rejection of mis-timed hits. This fact leads to two conflicting effects in terms of overall good performance:

1. the time resolution is very good for the isolated signal (hit in low luminosity conditions);
2. genuine hits in the same conditions which are slightly mis-timed are more likely to be rejected than in the case of a weighted sum processing.

In other words: when the time distribution of the genuine hits is narrow we can make optimal use of the comparator based filters, but as the distribution gets wider the weighted sum processing becomes more effective. This is clearly shown by the results obtained with the set of simplified signals, whose timing distribution enhances greatly the contribution of mis-timed events as a consequence of which the efficiency of the comparator based filters does not exceed 90%, while with the weighted sum it reaches 100%.

Another thing that can be observed is that the efficiency gradient with threshold appears to be more pronounced for the comparator based filters. The effect is more clearly visible in Figure 7. and it is mostly a consequence of what is stated in note 2, section 5. It is not excluded that appropriate moltiplicative factors for the thresholds could alleviate the effect.

The results shown at this stage for the beam test signals are obtained processing the signal which would be formed if the charge from the four channels was collected on one strip only; therefore they are only indicative of the trend of performance of the different filters. Results for the single channels are reported in section 6.3 and they will be used to quantify this effect.

6.2 Signal Gain

Figure 8 shows that the results obtained with the different sets of data are in agreement within less than 4%, except for the filter identified WUP23 where the maximum difference is 6%. Therefore I used the average of the three values obtained at σ=3 for the weighted sum filters and σ =1 for Peak and Edge finding (see note 2 in section 5) to estimate the effect of the different signal processing methods on the signal to noise ratio. This estimate, which takes into account the loss of signal as specified above and the contribution to the front-end electronic noise reported in Tables 1 and 2 is summarized in Table 3.

Figure 9 shows the pulse height spectrum in the case of the Monte Carlo signals before and after processing with three different filters. The spectrum relative to the Peak finding is obtained assuming that the analogue output is always present, regardeless of the algorithm response, and it consists of the sample at the peak. The ratio of the most probable values of the distributions after and before the processing has been calculated for all the methods and the results are in perfect agreement with those reported in Table 3.

6.3 Beam Test Data: Individual Channels

I used the beam test data to study in more detail the behaviour of the different filters in a more realistic environment, although still very far from the LHC environment. I evaluated the effects of noise on the efficiency (since noise was not considered in the simulated signals), the performance in presence of small signals (which can be also thought of as the effect of a drastic change in signal to noise) and the effect of noise on the occupancy.

Results are presented for the channel collecting most of the charge (channel 2) and the channel collecting the least charge (channel 1).

6.3.1 Channel 2 Results

The pulse height spectrum for channel 2 indicates a S/N=23 and a 3σ cut yields 57% of the total number of triggers (see Figure 5). Figure 10a shows the results relevant to this case.

It can be observed that the fraction of events which pass a 3σ cut for the weighted sum processing and a 1σ cut for the Peak finding is ~57% indicating approximately that the processing is fully efficient. The Edge sensing method is not fully efficient at 1σ (but the loss may be recovered by conveniently tuning the hardware comparator threshold).

Based on this result I choose these values of threshold as indicative of full efficiency and, in order to study the effect of a excursion in the front-end noise, I calculate the efficiency and fake hits rate excursion in a 2σ window around them. These values, reported in Table 4, represent the estimated effect on the processing performance of a 1σ excursion of the front end noise in either direction.

These numbers can be interpreted from two different points of view:

- from an operational point of view they indicate that a comparator based configuration requires a more accurate calibration than a weighted sum system;

- from the point of view of the implementation it demands, again for the Peak and Edge filters, the possibility of setting one individual threshold per chip. In fact the spread of the noise within one chip is thought to be limited to a few percent, but larger variations which might occur between different chips could severely affect the uniformity of efficiency across different modules[3]. This is not relevant for the weighted sum methods, since at the stage of the first zero suppression (Front End Driver), a different threshold is downloadable for each channel.

Figure 10b shows that the values of signal gain do not differ significantly from those reported in previous sections.

6.3.2 Channel 1 Results

From the pulse spectrum in Figure 5 we calculate a S/N=7 and a 3σ cut yields 9% of the total number of triggers.

Again, cutting at 3σ on the signal processed with the weighted sum methods, we recover the same fraction of events (figure 11a). The Peak finding at threshold 1σ shows a higher efficiency, indicating that this method picks up noise hits. This will be confirmed by the results shown in the next section, but could be avoided modifying slightly the algorithm. Edge sensing performance is again slightly inferior.

Applying the same considerations as in the previous section, I quantified the efficiency and fake hits rate excursion for a 2σ noise fluctuation and the results are in Table 5. Even if the number relative to the peak finding is inflated by the noise contamination mentioned above, we can draw the same, if not stronger, conclusions as in the previous section.

The signal gain (figure 11b) for the weighted sum filters is again consistent with the previous estimates. Instead both Peak and Edge finding show a consistent loss of signal (Edge>10%, Peak~35%). This effect is due partially to the noise contamination in the sample of tagged events, partially to the cross-talk effect which alters the shape of the signals and partially to the intrinsic difference in the time evolution of small and large signals; the sampling time has been, in fact, optimized for best performance of the channel collecting the largest charge.

In case the use of the Peak or Edge sensing filter is considered it is important to verify that such distortion effect can be minimized, since a non-uniform response in terms of pulse height certainly affects the spatial resolution, most notably with inclined tracks. No data are available at the moment for a further characterization of the effect, but we can surely reaffirm the key importance of an accurate calibration for the these methods.

6.3.3 Effect of Noise on the Occupancy

In order to quantify this effect I processed with the different filters a sample of 1000 events of pure noise recorded with the PRESHAPE32 during the calibration of the test beam setup. It should been remarked that the average pulse shape for the 1000 events examined presents a small bump whose timing is consistent with the peaking time of the amplifier. This fact suggests that these events could contain some small fraction of signals from particles. The noise distribution is shown in Figure 5 and the occupancy at different thresholds after processing is reported in Table 6.

The occupancy at 3σ is less than 2% before processing and after the weighted sum filters; at 1σ it is slightly higher than 3% for the Edge sensing and 14% for the Peak sensing method. This last value reflects what was

---

[3] Larger variations within one group of channels read out by one chip are expected after the modules assembly is completed

mentioned in the previous section. A slight modification of the Peak algorithm will cut the noise contamination to an acceptable level, namely the addition of a discrimination between the output signal and the electronic noise. This translates to adding to Table 2 the additional condition: $V_n > c*\sigma$ with *c* a constant to be determined. This could be a software rather than a hardware threshold.

A preliminary study, however, shows that the determination of the constant is not a trivial problem. In fact this cut is used to ultimately discriminate signal from noise, whatever the signal size. Small signals will suffer if a good noise rejection is achieved. In fact when the charge is shared by several strips or in the case of inclined tracks, often the genuine signal is well hidden amongst the noise and only dedicated hit finding and clustering algorithms are effective in tagging it.

With the data examined, c=3 yields a noise occupancy of 0.3%; c=0 yields 7%.

The correspondent efficiencies for the genuine signals on Channel 1 are 0.5% (c=3) and 6% (c=0).

6.4 Effect of Pile-up on Processing

The piling-up of signals from different bunch crossings generates a distortion of the signal shapes which affects the processing performance. One would qualitatively expect the two comparator based methods, which rely heavily on the shape of the signal, to be affected to a greater extent.

I investigated briefly this effect using the simplified signals. I let two identical events happen, separated in time for 1 up to 5 BCI. I then plotted the output signal amplitude (normalized to the input) after the threshold cut for both the events.

Results are reported in Figure 12 and they confirm what was expected. With all the weighted sum methods we would tag both events if they were both associated to a trigger. The analogue amplitude is distorted for one of the two events, except in the case of the WUP2 filter, for which the distortion is appreciable only in the case of back to back events. Of the two events, the Peak and Edge methods would fail to tag the one associated with the second trigger, while the analogue output amplitude is heavily inflated for the event associated with the first trigger, indicating a degradation of performance with increasing occupancy. To evaluate this effect more fully a wider range of amplitudes and occupancies representative of real data need to be considered . This should be taken as a preliminary indication of the “consequence of pile-up”.

7 Summary

Different factors need to be taken into account in order to make the best choice, as none of the algorithms is a clear winner in every aspect.

- Hardware issues:

  1) number of weights (physically capacitors) to be used; it should ideally be minimized;

  2) number of samples reserved and their distance in the pipeline affects both the front-end chip dead-time and the complexity of the APSP logic to be implemented;

  3) presence or not of hardware threshold.

- Performance requirements:

  1) optimal combination of efficiency and time resolution for an isolated trigger;

  2) effect on occupancy should be minimized;

  3) minimum degradation of S/N

  4) efficiency for consecutive triggers should be maximized

The relevant quantities, as estimated in this study are summarized in Table 7.

One further consideration concerns the existence of common mode noise in the system. This fact demands that the analogue values being preserved in order to perform the subtraction at the Front End Driver level. This is relevant to the comparator based systems, which were originally conceived to suppress the signal if the algorithm condition was not satisfied. This should be avoided and all the analogue values should be output, accompanied by a flag indicating the response of the processing.

8 Conclusions

A number of analogue signal processing algorithms for MSGCs signals in CMS have been assessed using three different sets of data (simulated and from a beam test) with the purpose of indicating the most suitable for the implementation in the APV front end chip. Performance has been evaluated in different scenarios in order to ensure the reliability of the filtering process. The results obtained with the three methods are in good agreement and 6 out of the initial 15 algorithms under test consistently show a superior performance: one of Peak sensing type, one Edge sensing and four Weighted Sum filters.

If a detector system which ensures long term stability of operating conditions and occupancy is foreseen, a peak or edge sensing algorithm could be preferred. Some comments, however, need to be made.

The system stability, to guarantee stability in the time evolution of the signals collected at the front end, is of primary importance since the method relies heavily on the shape of the amplified signal. The occupancy itself is not influenced to a great extent by the these filters, but, as it rises, the performance of the methods degrades.

Some difficulties could arise in the process of calibrating accurately ~60000 readout chips in the system during the detector lifetime, as the algorithms are extremely sensitive to threshold changes. An additional problem comes from the fact that, according to the readout scheme foreseen for CMS (analogue), the analogue values must be preserved for all channels, regardless of the algorithm response. This gives the additional advantages of facilitating the monitoring of the system and allowing to perform common noise subtraction. A scheme for achieving this does not yet exist.

Besides this, additional issues still need to be investigated. They concern the capacity of the method to discriminate efficiently signal from noise in the case of small signals and the linearity of the analogue response over the whole range of amplitudes expected.

The Weighed Sum filters have shown to provide more robust data handling (section 6.1). Therefore, if stable detector operating conditions cannot be guaranteed, one of the Weighted Sum filters would represent the best solution. The method is simple to implement and a similar system has already been prototyped on the APV6 front end chip for the silicon microstrip detectors.

Advantages are the experience already existing with the APV6; the lack of need of any additional calibration procedure; the overall consistency of performance throughout different scenarios which ensures robustness against detector system instability.

Drawbacks are an increased occupancy, which in itself does not turn out to affect the performance of the filters, and a reduced final signal to noise ratio.

Four sets of weights have been proved to a certain performance; further optimization of the values could bring slight improvements for both occupancy and signal to noise ratio.

The final choice will also depend on the hardware requirements summarized in the previous section and operational issues in the CMS framework which are not discussed in this paper.

Acknowledgements

I would like to thank Mark Raymond for the constructive discussions, Geoff Hall for continuous advice and assistance, Martin Millmore for invaluable help with software, Mario Spezziga for providing the Monte Carlo signals and Jean F. Clergeau for providing the data relative to the beam test.

References

[1] **IEEE Trans. Nucl.Sci. NS-41 (1994) 1086**, G. Hall.

[2] **CERN/DRDC 94-39 (1994)**, RD20 Status Report

[3] **Nucl. Instr. and Meth. A 326 (1992) 112**, N. Bingefors et al..

[4] **Nucl. Instr. and Meth. A 320 (1992) 217,** S. Gadomski et al..

[5] **CERN/LHCC/95-96 (1995)** 120, M. French et al., Proceedings of the first workshop on electronics for LHC experiments, Lisbon 95..

[6] **INFN PI/AE-94-02 (1994)**, R. Bellazzini, M.A. Spezziga, "*Electric Field, Avalanche Growth and Signal Development in Micro-Strip Gas Chambers and Micro-Gap Chambers*"

[7] **CMS TN/94-215**, R. Sachdeva, "*Signal Processing for MSGCs at CMS*"

[8] S. Snow, "*Comparison of Algorithms for Associating an MSGC Signal to a Beam Crossing Interval in ATLAS*" Manchester University Preprint (1994).

[9] L. Jones, "*A 64 channel Analogue Pipeline Integrated Circuit for MSGCs -- MARS*," RAL Preprint (1995).

[10] **NIM A 368 (91996) 345-352,** F. Angelini et al..

[11] **CMS NOTE/97-013**, J.F. Clergeau et al., "*Proposal for the Read-out Electronics of Gas Micro Strip Detectors in the CMS Tracker*"

OUTPUT Ws=S Wi*Vi if: trigger		
Algorithm designation	Weights Wi	Series Noise Factor
WUP1	1.213 -1.471 0.446 0	1.51
WUP2 *	1.213 -0.258 -1.025 0.446	1.53
WUP22 *	1.213 -0.258 -1.025 0	1.6
WUP23 *	1.213 0.105 -1.102 -0.307	1.76
WUP3	1.516 -2.181 0.84 0	2.12
WUP4	1.516 -0.665 -1.342 0.84	2.04
WBP1	1.064 -0.209 -2.025 1.431	2.29
WBP2	1.037 -0.155 -1.717 1.066	1.95
WTP1	-0.047 1.491 -2.075 0.788	2.02
WTP2	-0.119 1.596 -2.118 0.792	2.08
WS	1 -0.5 -0.84 0.43 0.14	1.51
DC1 *	1, 0, -1, 0	1.41
DC2	1, -1, 0, 0	1.18

Table 1. Details of weights used for the weighted sum algorithms.
"*" denotes those whose results are shown in the paper

OUTPUT: Vn if: trigger & condition is true		
Algorithm	Condition	Series Noise Factor
Edge Finding *	$(V_n-V_{n-3})>3\sigma$ $(V_n-V_{n-2})>\sigma$ $(V_{n-2}-V_{n-3})>\sigma$	1
Peak Finding *	$(V_n-V_{n+2})>\sigma$ $(V_n-V_{n-2})>\sigma$	1

Table 2. Details of the edge finding and peak finding algorithms.
V_n = sample at BCI n; $V_{n\pm i}$ = samples at BCI n±i

Algorithm	Signal Gain (average)	Signal/Noise Loss (%)
WUP2	0.80	47.6
WUP22	0.80	49.9
WUP23	0.98	44.4
DC1	0.75	46.7
Edge Finding	0.97	3
Peak Finding	0.97	3

Table 3. Effect of the signal processing on Signal to Noise ratio.

Algorithm	Efficiency excursion (%) for a 2 σ threshold shift	Fake Hits Rate excursion (absolute) for a 2 σ threshold shift
weighted sum	6.7	3.2 (from 4.5 to 1.3)
Edge Finding	12	0.4 (from 0.6 to 0.2)
Peak Finding	14.5	0.4 (from 0.6 to 0.2)

Table 4. Effect of a 2 σ threshold shift on the processing performance for Channel 2.

Algorithm	Efficiency excursion (%) for a 2 σ threshold shift	Fake Hits Rate excursion (absolute) for a 2 σ threshold shift
weighted sum	20	3.2 (from 3.5 to 0.3)
Edge Finding	54	0.6 (from 0.8 to 0.2)
Peak Finding	65	0.6 (from 0.8 to 0.2)

Table 5. Effect of a 2 σ threshold shift on the processing performance for Channel 1.

sigma	CRRC	WUP2	WUP22	WUP23	DC1	EDGE	PEAK
0	0.459	0.49	0.516	0.509	0.504	0.186	0.341
1	0.185	0.247	0.22	2.227	0.219	0.033	0.143
2	0.054	0.079	0.068	0.07	0.068	0	0.046
3	0.013	0.018	0.014	0.009	0.012	0	0.009
4	0.002	0.003	0.003	0.001	0.004	0	0.002
5	0	0	0	0	0.	0	0.001
6	0	0	0	0	0	0	0

Table 6. Noise occupancy after signal processing.

Algorithm	n. weights	n. Samples	hard THR	efficiency	fake hits rate	S/N loss	noise occ.
WUP2	4	4	no	96%	2	47.6%	1.8%
WUP22	3	3	no	96%	2	49.95	1.4%
WUP23	4	4	no	96%	2	44.4%	0.9%
DC1	2	2	no	96%	2	46.7%	1.2%
Peak	4	3	yes	94%	0.5	3%	7.3% *
Edge	6	3	yes	94%	0.5	3%	3.3%

Table 7. Summary of the quantities relevant to the choice as estimated in this study.

*) Obtained with an additional cut (V_n>0); see section 6.3.3.

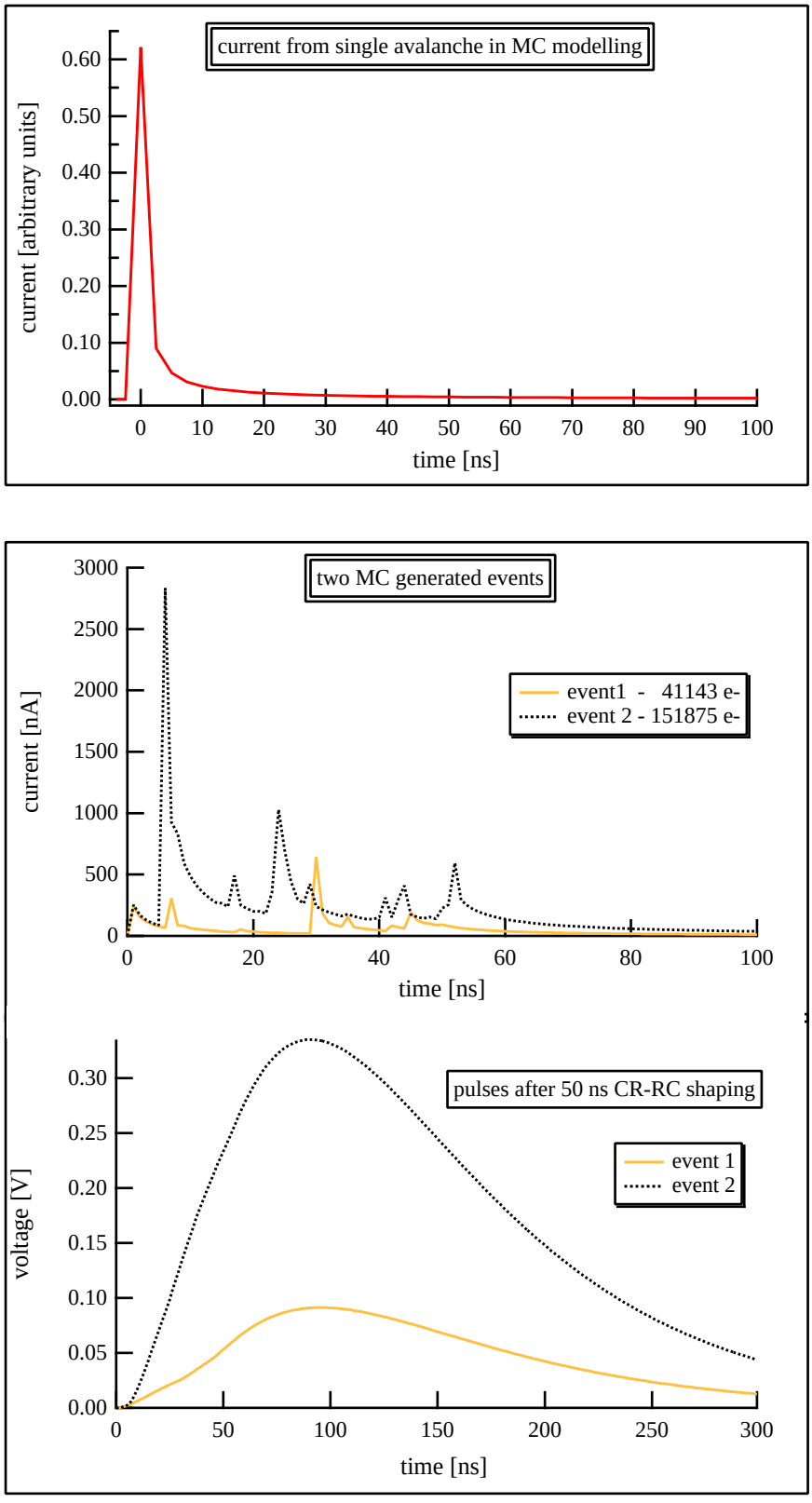

Figure 1. Simulated current signal from a single avalanche (top). Two simulated events (bottom): current signals and pulse after a 50 ns shaping.

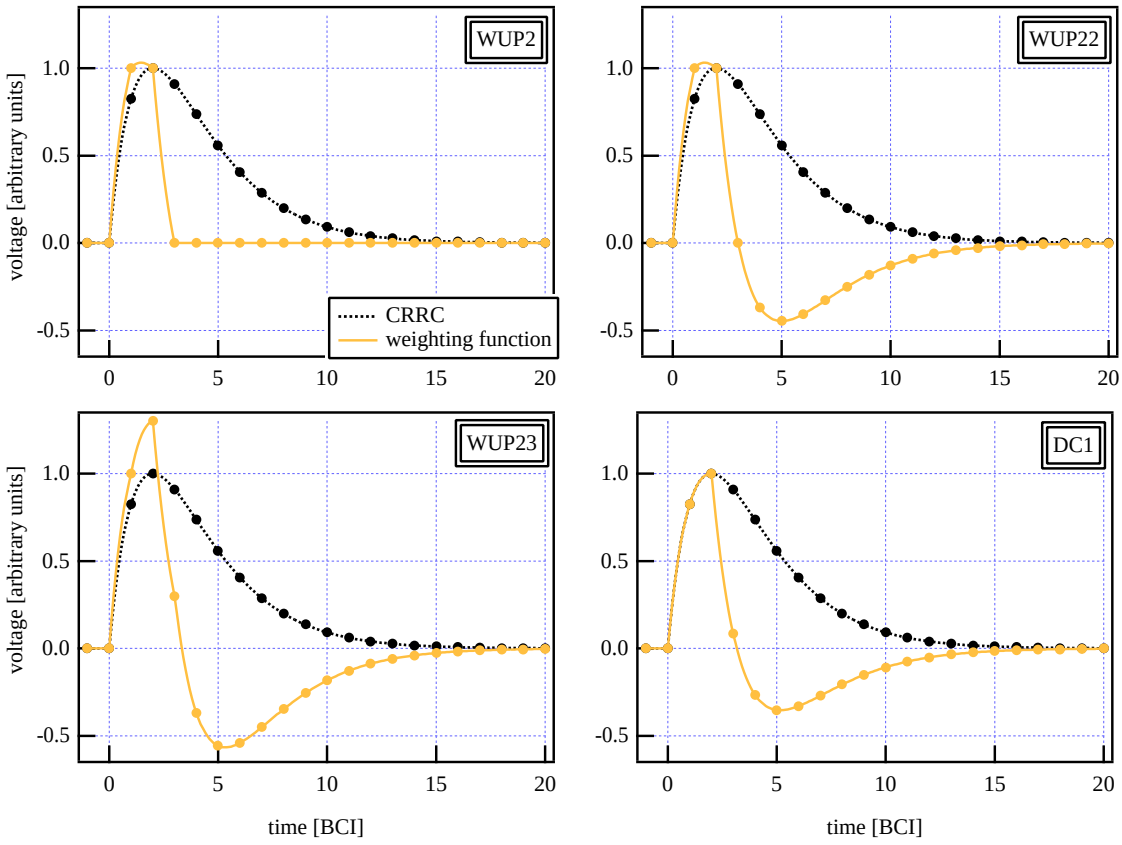

Figure 2. Weighting function for some of the weighted sum algorithms considered

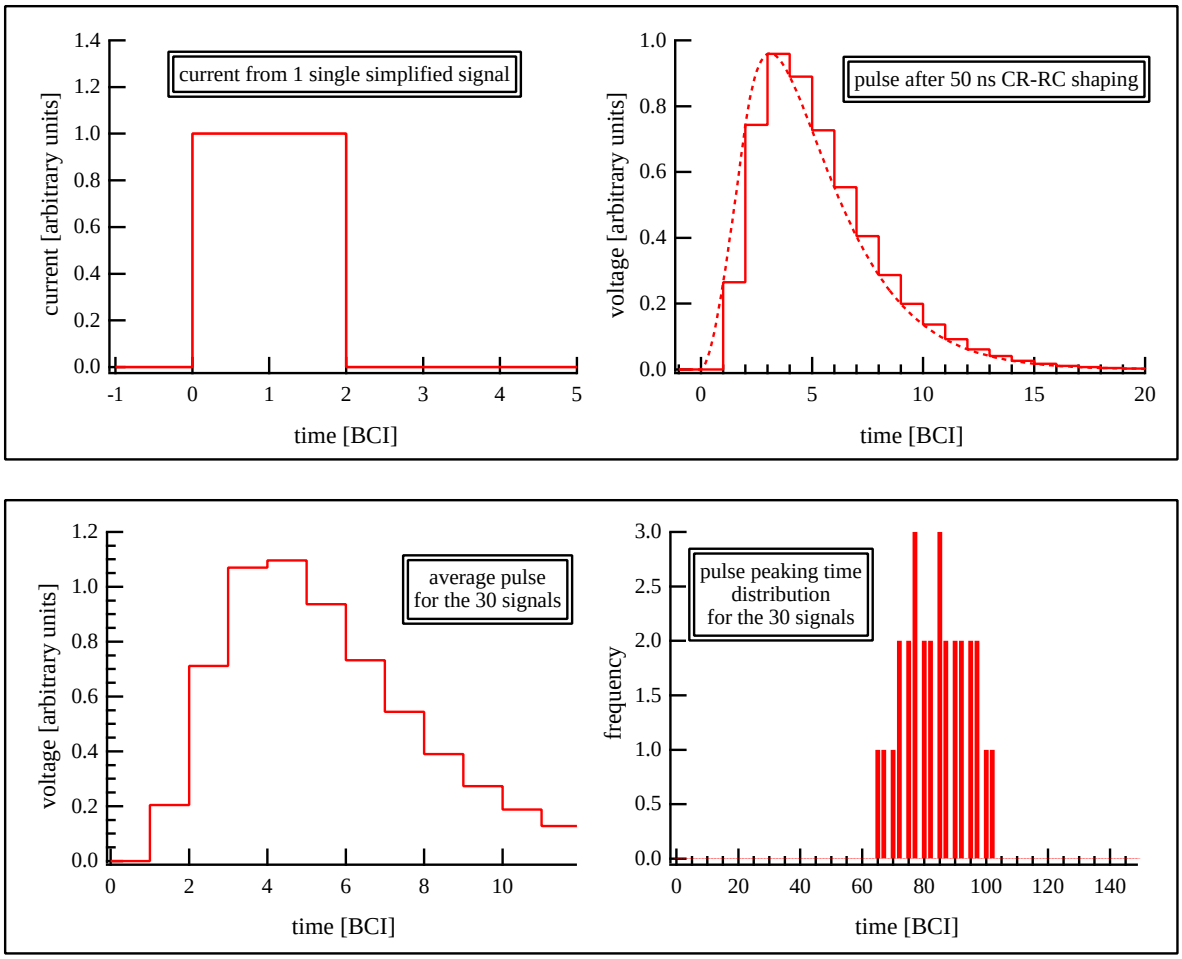

Figure 3. Simplified simulated signals.

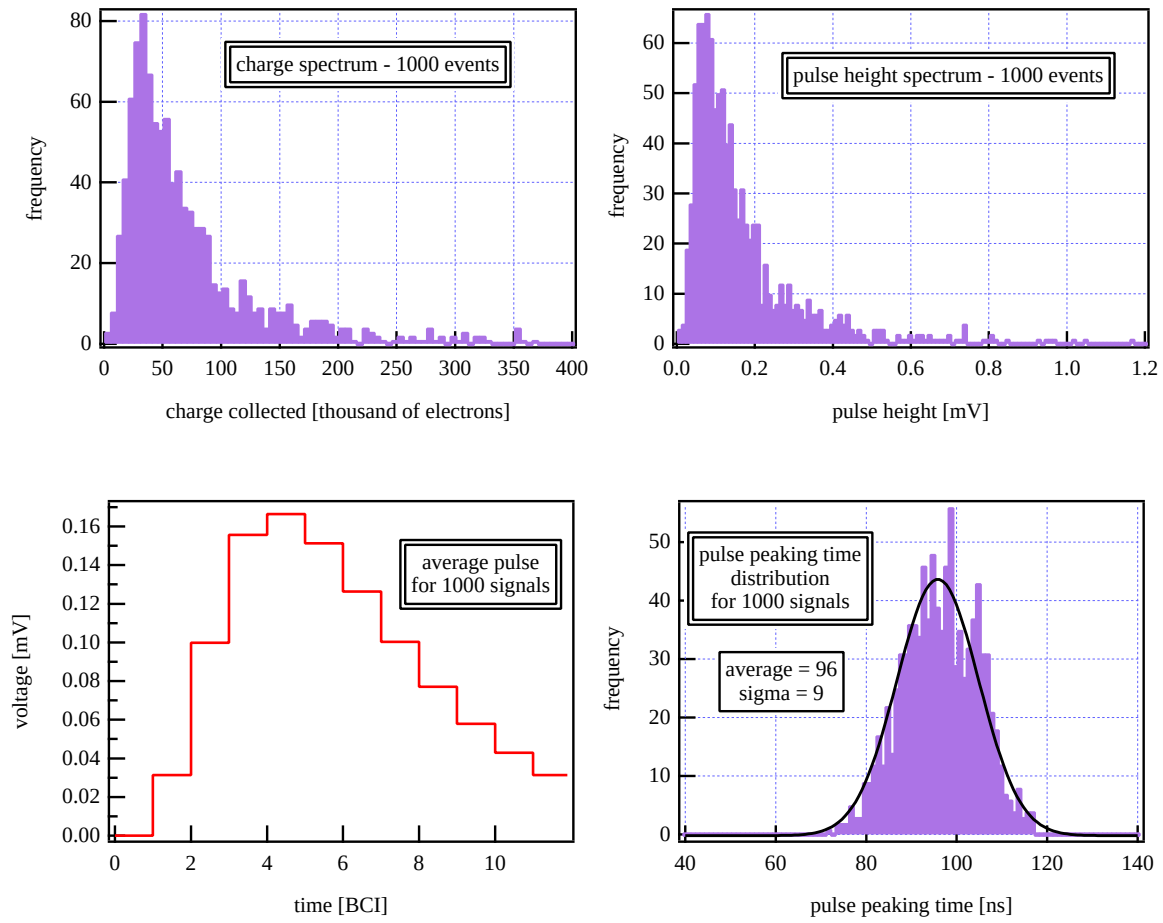

Figure 4. Realistic simulated signals.

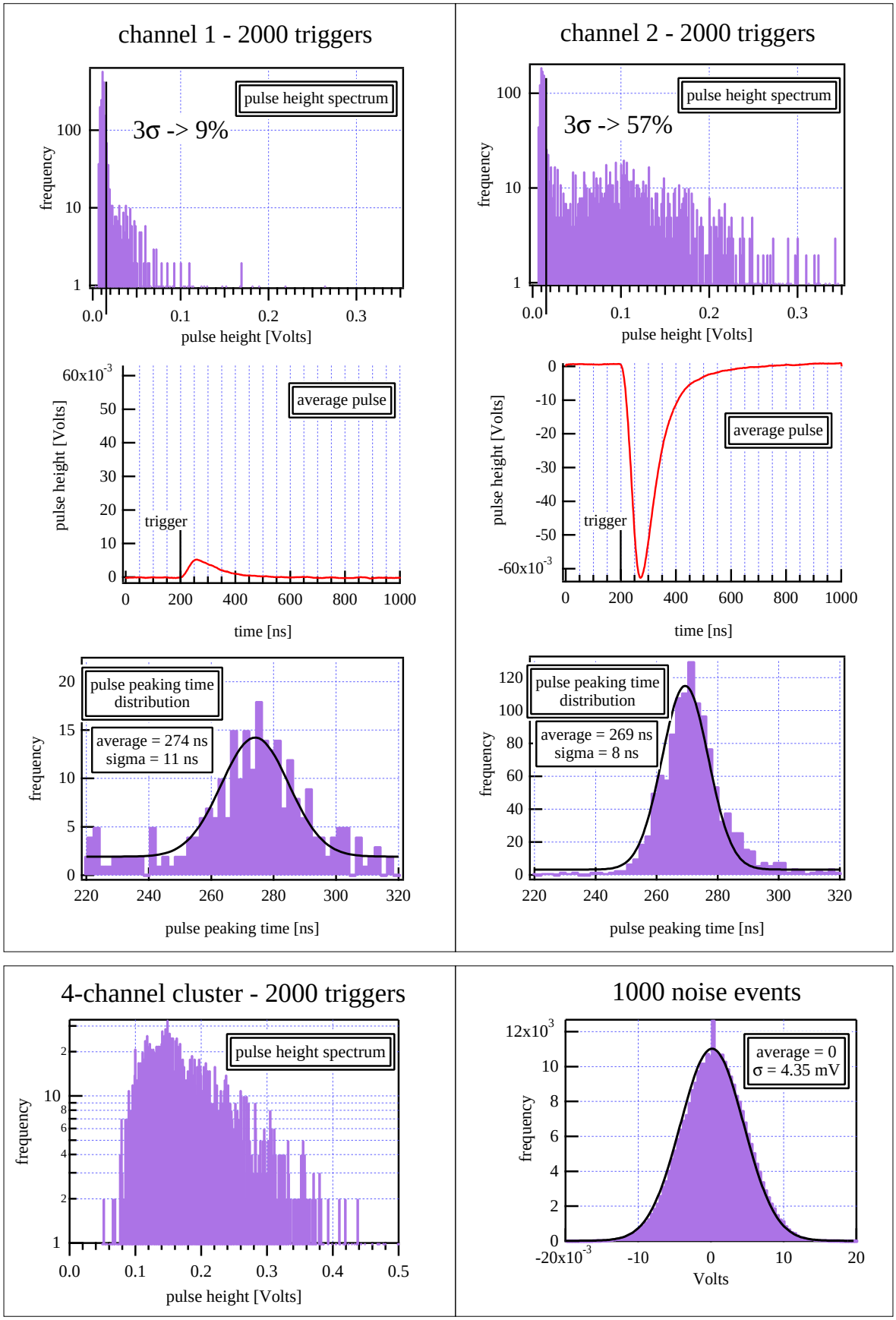

Figure 5. Signals from a beam test. The distributions for Ch. 3 and Ch. 4 are similar respectively to those of Ch. 2 and Ch. 1.

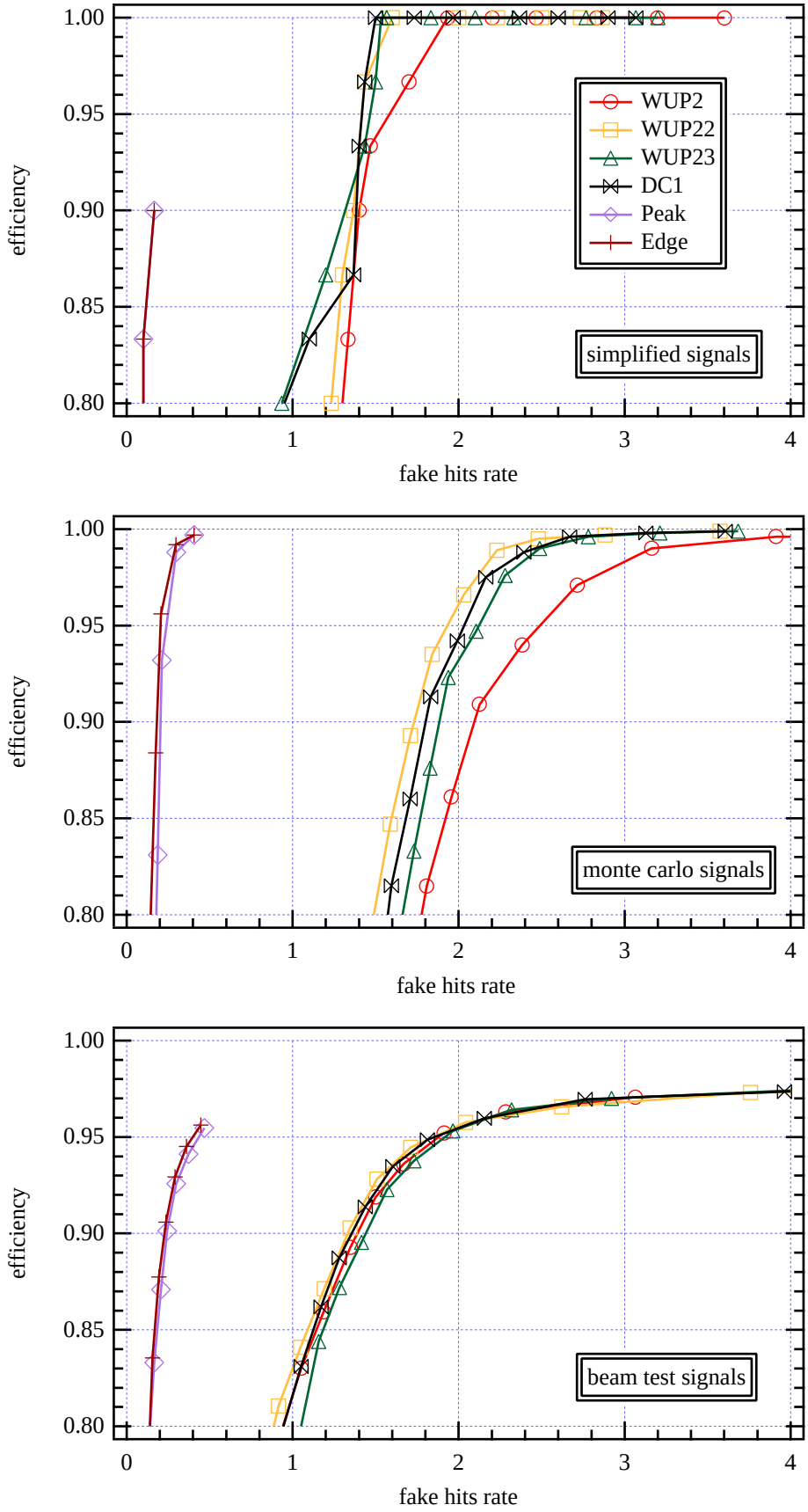

Figure 6. Efficiency vs Fake Hits Rate for the three sets of data.

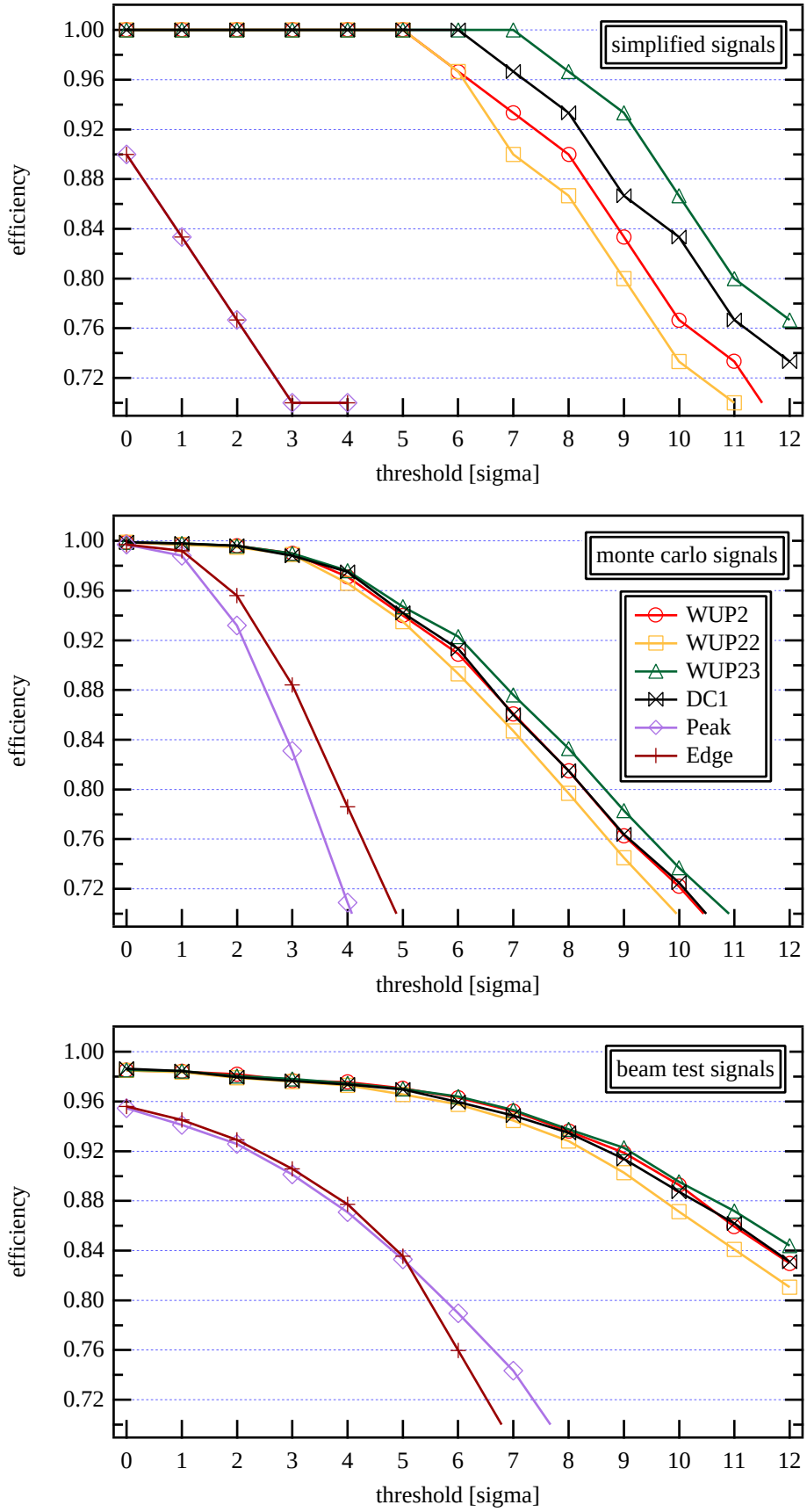

Figure 7. Efficiency as a function of threshold.

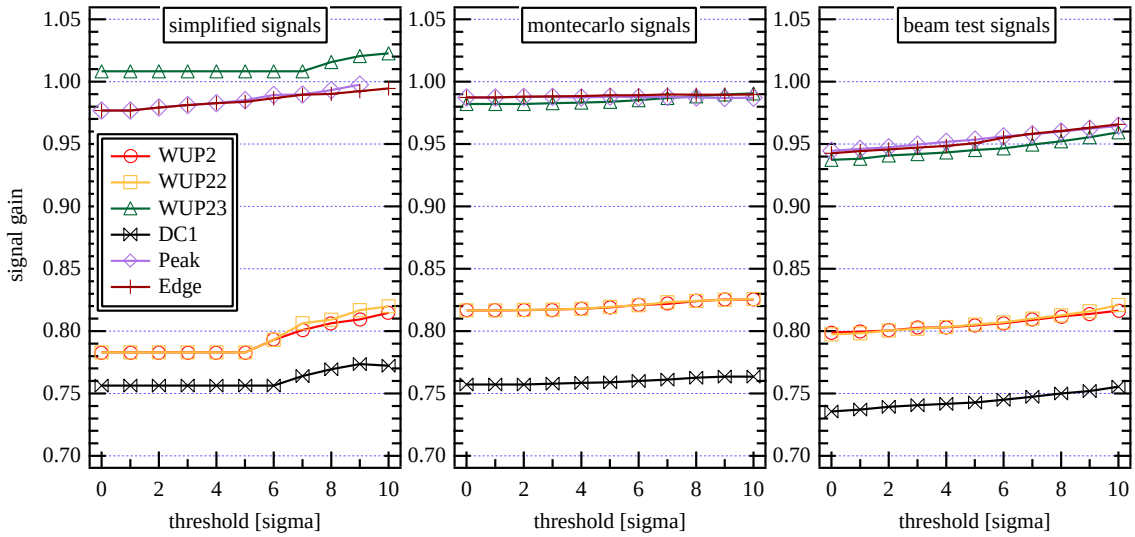

Figure 8. Signal gain with the three different sets of data.

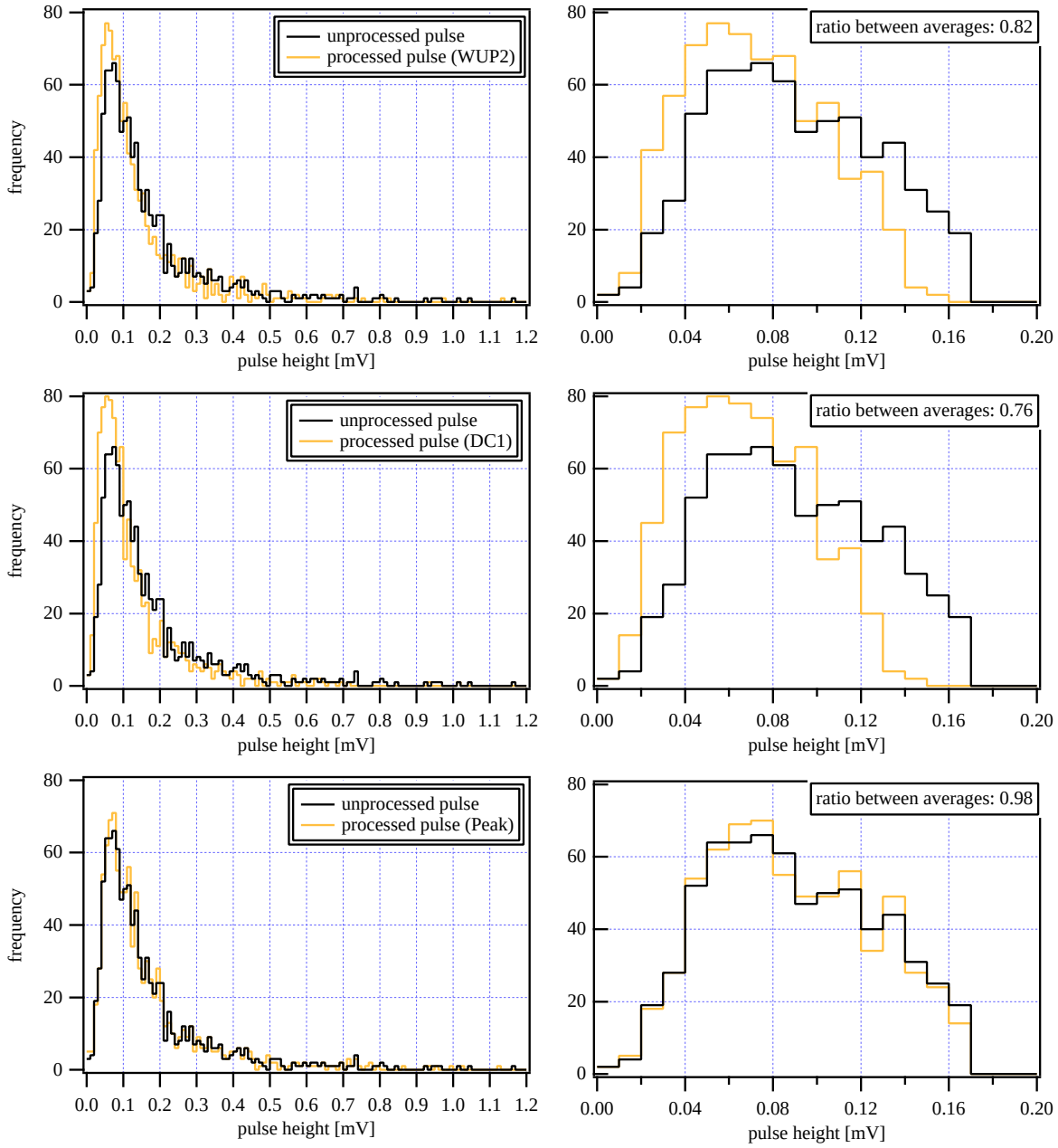

Figure 9. Pulse height spectrum before and after processing for the realistic simulated signals. The plots on the right show the region of the most probable signal.

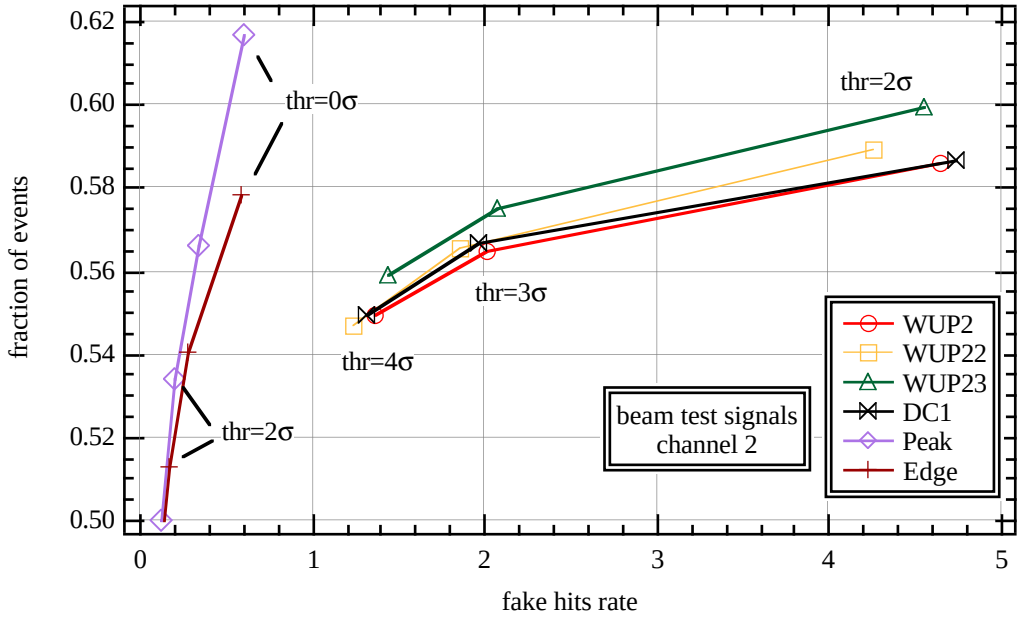

Figure 10a. Efficiency vs Fake Hits Rate for beam test data - Channel 2.

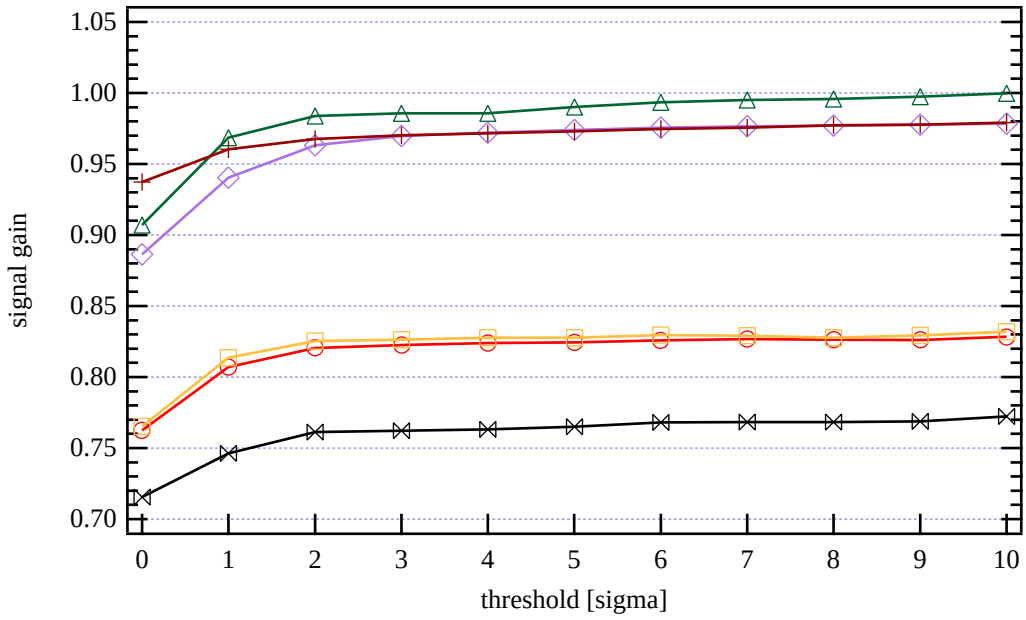

Figure 10b. Signal Gain for beam test data - Channel 2.

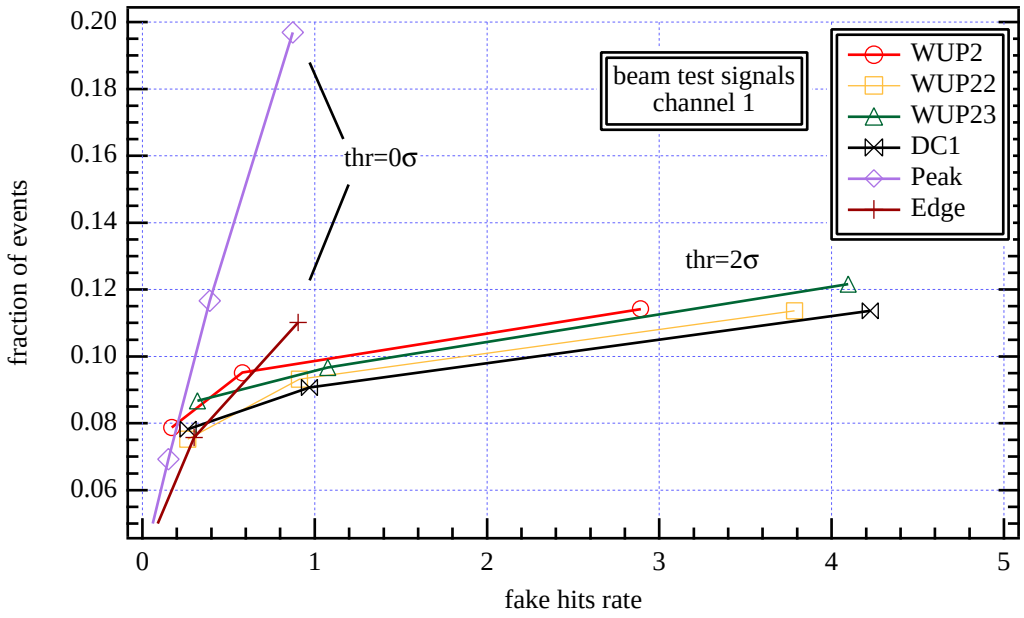

Figure 11a. Efficiency vs Fake Hits Rate for beam test data - Channel 1.

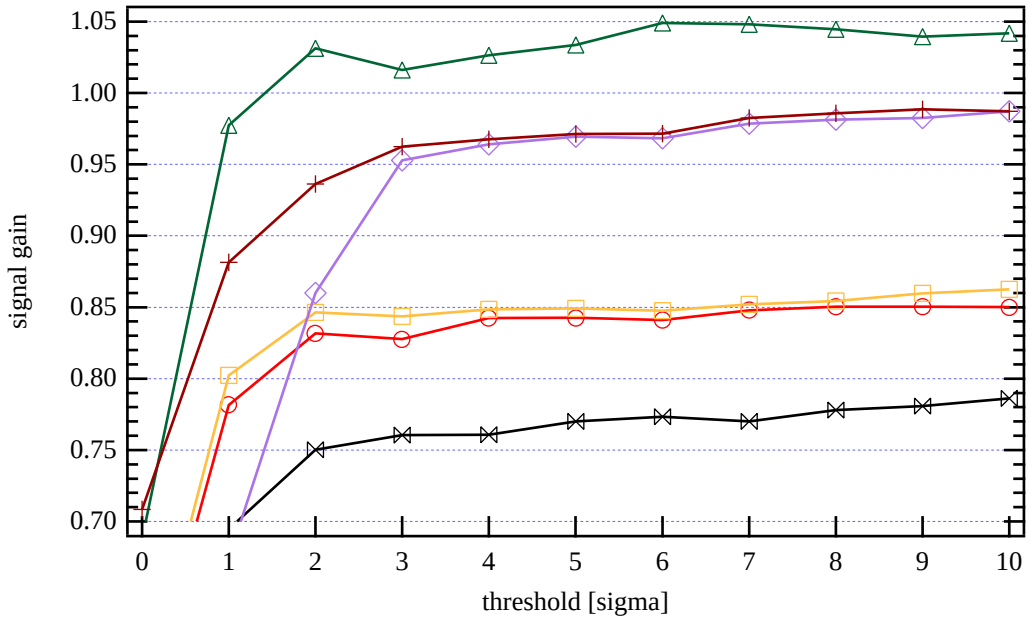

Figure 11b. Signal Gain for beam test data - Channel 1.

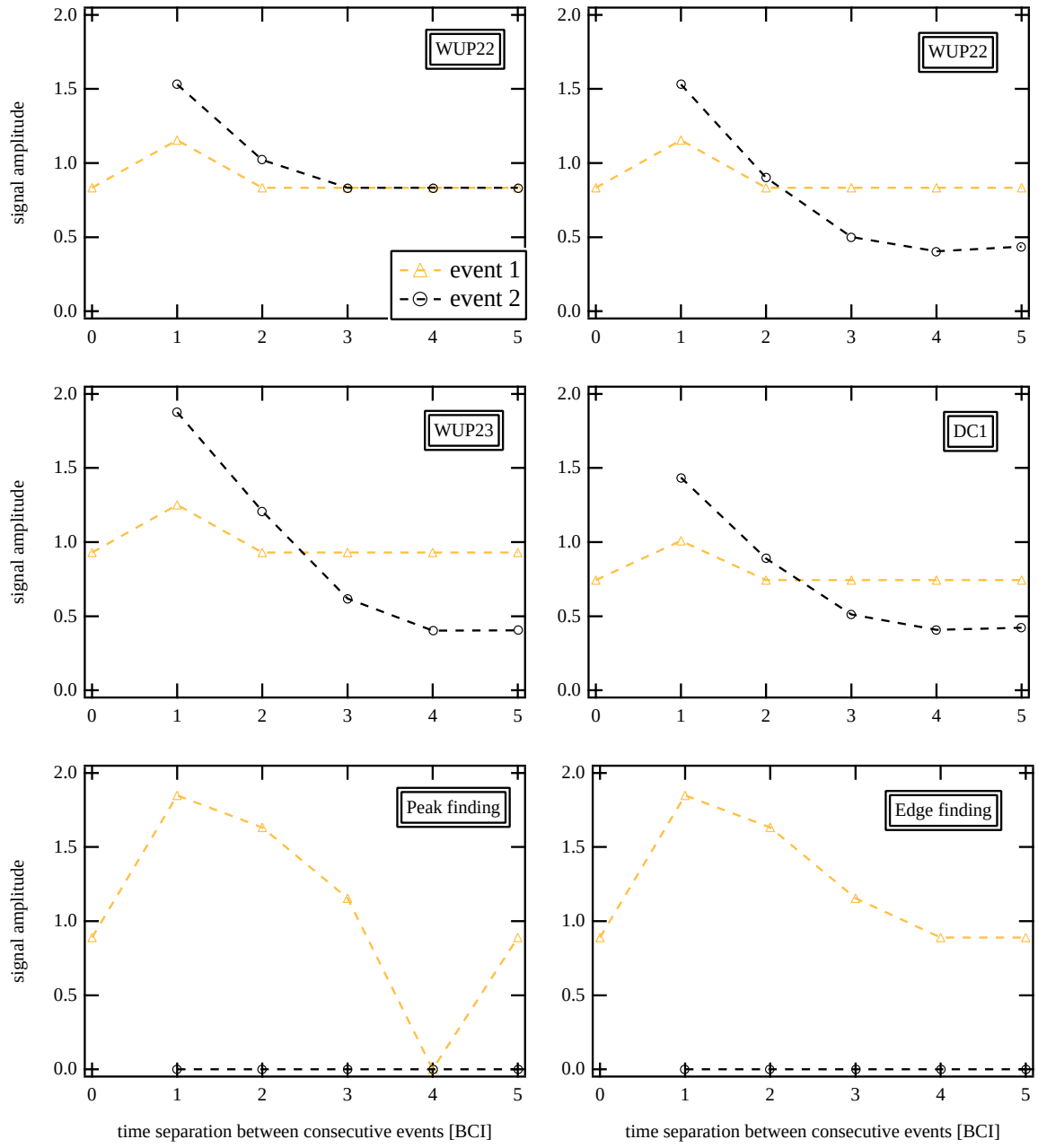

Figure 12. Processing response in the case of two consecutive events as a function of the separation in time between them